SCIENTIFIC REPORTS

OPEN

SUBJECT AREAS:
METAL-ORGANIC FRAMEWORKS
HYDROLASES
BIOCATALYSIS

Received
18 July 2014

Accepted
6 October 2014

Published
24 October 2014

Correspondence and requests for materials should be addressed to B.L. (libin36@ynu.edu.cn) or J.W. (jqwang@ynu.edu.cn)

MOFzyme: Intrinsic protease-like activity of Cu-MOF

Bin Li, Daomei Chen, Jiaqiang Wang, Zhiying Yan, Liang Jiang, Deliang Duan, Jiao He, Zhongrui Luo, Jinping Zhang & Fagui Yuan

Yunnan Engineering Research Center of Photocatalytic Treatment of Industrial Wastewater, The Universities' Center for Photocatalytic Treatment of Pollutants in Yunnan Province, Key Laboratory of Medicinal Chemistry for Natural Resource, Ministry of Education, School of Chemical Sciences & Technology, Yunnan University, Kunming 650091, P.R. China.

The construction of efficient enzyme mimetics for the hydrolysis of peptide bonds in proteins is challenging due to the high stability of peptide bonds and the importance of proteases in biology and industry. Metal-organic frameworks (MOFs) consisting of infinite crystalline lattices with metal clusters and organic linkers may provide opportunities for protease mimic which has remained unknown. Herein, we report that $Cu_2(C_9H_3O_6)_{4/3}$ MOF (which is well known as HKUST-1 and denoted as Cu-MOF here), possesses an intrinsic enzyme mimicking activity similar to that found in natural trypsin to bovine serum albumin (BSA) and casein. The Michaelis constant (K_m) of Cu-MOF is about 26,000-fold smaller than that of free trypsin indicating a much higher affinity of BSA for Cu-MOF surface. Cu-MOF also exhibited significantly higher catalytic efficiency than homogeneous artificial metalloprotease Cu(II) complexes and could be reused for ten times without losing in its activity. Moreover, Cu-MOF was successfully used to simulate trypsinization in cell culture since it dissociated cells in culture even without EDTA.

Artificial enzyme mimetics have become an increasingly important focus for research, because natural enzymes bear some considerable disadvantages, such as a sensitivity of catalytic activity in environmental conditions, a relatively low stability and a poor recovery[1,2]. In such context, many nanomaterials, such as fullerene derivatives[3], gold nanoparticles[4,5], rare earth nanoparticles[6] and ferromagnetic nanoparticles[7–9], have been found to exhibit unexpected enzyme-like activity. Therefore the term "nanozymes" was initially coined by Scrimin, Pasquato and co-workers ten years ago[10,11]. Because many enzymes contain metal ions in the active site, synthetic metallopeptidases have been the subject of extensive research in the past decades, and important progress has been made[4,12–17]. For example, artificial active sites comprising the Cu(II) complex of cyclen (Cu(II)Cyc) and aldehyde group were synthesized on a cross-linked polystyrene to design artificialproteases[18]. $Cu([9]aneN_3)Cl_2$ was also used to hydrolyze Gly-Glyand bovine serum albumin (BSA) at near-physiological pH[12].

On the other hand, metal-organic frameworks (MOFs), a type of zeolite-like crystalline porous materials, have been extensively exploited in applications for gas storage, separation and catalysis because of their extremely large surface areas and wide variety of shapes and porosity[19–25]. Biological systems such as enzymes interact and function through multiple simultaneous interactions[26]. Therefore, it occurred to us that MOFs should be suitable to act cooperatively in a catalytic process of enzymes as those well-explored metal complexes[12–17]. Indeed, mesoporous MOF PCN-222(Fe) with porphyrinic Fe(III) centers[27], Fe(III)-based MIL-53[28], MIL-68 and MIL-100[29] were found to be effective peroxidase mimics. But so far, efforts devoted to the use of MOFs as adsorbents for peptide enrichment[30], protein conjugationor[31], or enzyme immobilization[32–37] are still limited. Although enzymes such as microperoxidase-11[32], myoglobin[33], heme enzymes[34], hemin enzymes[35] and trypsin[36,37] have been successfully immobilized onto MOFs. The desirable features of MOFs have rarely been applied to an enzymatic mimic, let alone intrinsic enzyme-like properties and simulation of trypsinization in cell culture. In particular, the possibility of MOFs as intrinsic proteasemimic has remained unknown, though MOFs continuously attract many researchers to explore their unparalleled potentials for a wide range of applications.

Trypsin was chosen as a model because it is the most commonly used proteolytic enzyme for protein digestion and transformation into peptides for proteomics studies as well as for industrial production[36]. Moreover, designing enzyme-like catalysts for the hydrolysis of the peptide bonds of proteins is challenging in view of the high stability of those bonds[18,38]. Herein, we show for the first time that Cu-MOF[21,39–43] ($Cu_2(C_9H_3O_6)_{4/3}$, also known as HKUST-1) possesses an intrinsic trypsin-like activity even without any chemical modification on the MOF

surface. For the simulation of trypsinization in cell culture, Cu-MOF was also used to dissociate Lung cancer A549 cells since trypsin-EDTA (ethylene diaminetetraacetic acid) has been widely used for subcultivation and scale-up of several cell lines, to detach cells from either static or carrier surfaces.

Results

Characterizations of catalyst. The X-ray diffraction (XRD) pattern of the as-synthesized Cu-MOF is shown in Supplementary Fig. S1. The diffraction peaks are all corresponded to the products synthesized by Klaus Schlichte[43] and the overall is agreement with a pattern calculated from crystallographic data in this reference. The textural properties of Cu-MOF have also been investigated by N_2 adsorption-desorption measurement (Supplementary Fig. S2, S3). The adsorption-desorption isotherm of Cu-MOF is of type I indicating the presence of the microporous network, which possesses a specific pore volume of 0.46 $cm^3\ g^{-1}$ and an average pore size of 1.95 nm. The Langmuir Surface Area (1261 $m^2\ g^{-1}$) and Brunauer-Emmer-Teller (BET) surface area (956 $m^2\ g^{-1}$) are shown in Supplementary Table S1. The particles size of Cu-MOF crystals revealed by Scanning electronic microscopy (SEM) is about 2 to 3 nm (Supplementary Fig. S4). According to the Fourier transform infrared spectroscopy (FT-IR) spectrum between 500 and 3800 cm^{-1} (Supplementary Fig. S5), the peaks at 730 and 1110 cm^{-1} could be assigned to the vibrations of the organic ligand (BTC, 1, 3, 5-Benzenetricarboxylic acid). The zone between 1300 and 1700 cm^{-1} is related to the carboxylate ligands and is thus indicative of the coordination of BTC to the copper sites[44]. More precisely, the bands at 1642 and 1590 cm^{-1} and at 1446 and 1371 cm^{-1} corresponds to the asymmetric and symmetric stretching vibrations of the carboxylate groups in BTC, respectively[45]. The peaks near 3423 cm^{-1} correspond to the stretching vibrations of the O–H linkage on the surface of the sample. All the results mentioned above confirmed that Cu-MOF was properly synthesized.

Proteolytic reaction catalyzed by Cu-MOF. Proteolytic activity of Cu-MOF was examined using BSA, a 66,000 Da protein, as the substrate. While the buffer solution containing a protein substrate (15 μM) was shaken with Cu-MOF, disappearance of the protein was observed by sodium dodecyl sulfate polyacrylamide gel electrophoresis (SDS-PAGE)[46,47]. Measurement of the total amino acid content of the product solution separated from Cu-MOF by centrifugation confirmed that the disappearance of the electrophoretic band of BSA was not due to the adsorption onto the catalyst[48]. It was observed that BSA was hydrolyzed by Cu-MOF at 37°C and pH 9.0. Although hydrolysis was very weak, many fragment bands appeared with the molecular weights of approximately 55, 40, 32, 25, 15 and 12 kDa after 30 min (see Supplementary Fig. S6). The intensities of BSA bands reduced slowly within five hours, which means the catalytic activity of Cu-MOF was very weak at 37°C. The intensities of these fragment bands were also very low, indicating that the observed fragments were intermediary products and further hydrolysis proceeded during the reaction. Nevertheless, Cu-MOF acted as the digestion enzyme and cleaved BSA. Temperature and pH values are crucial factors that affect the digestion results. We found that pH 9.0 was suitable for the reaction (Supplementary Fig. S7). The catalytic activity was influenced more significantly by temperature at a lower pH. When the temperature was raised from 37°C to 50°C, the intensities of BSA bands reduced and discrete polypeptides appeared after 10 min (Fig. 1a). Then BSA was further cleaved with time, resulting in a significant loss in intensity of the BSA band. When BSA was incubated at 70°C, it was cleaved into a myriad of fragments, resulting in a significant loss in intensity of the BSA band and a concomitant smear on the SDS-PAGE gel. The band of BSA disappeared after 15 min, which revealed the enhancement of the digestion activity at 70°C (Supplementary Fig. S8).

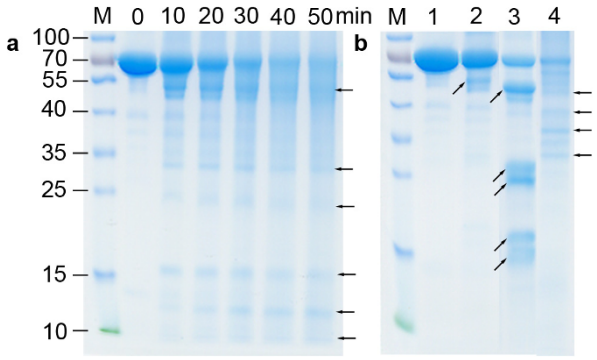

Figure 1 | BSA cleaved by Cu-MOF or trypsin. (a) Results of SDS-PAGE performed on BSA (15 μM) incubated with Cu-MOF (0.99 mM) at pH 9.0 and 50°C. (b) BSA incubated with trypsin (40 : 1 w/w) and Cu-MOF (0.99 mM) at pH 7.4 for 20 min. Lane 1: BSA solution reacted at 70°C as control group (without trypsin and Cu-MOF). Lanes 2–3: BSA reacted with trypsin at 70°C and 37°C, respectively. Lane 4: BSA incubated with Cu-MOF at 70°C.

Unsurprisingly, large amount of BSA could still be digested in this harsh condition. By contrast, there was only a fragment with the molecular weight of approximately 55 kDa appeared at 70°C and pH 7.4 (lane 2, Fig. 1b), which illustrated the activity of trypsin was inhibited significantly at high temperature. For Cu-MOF, the four bands of protein with 55, 40, 37 and 32 kDa can be observed at 70°C and pH 7.4 (lane 4, Fig. 1b). This implied that the activity of Cu-MOF was not affected by the high temperature indicates that Cu-MOF possesses a better heat-resistance than free enzymes.

A typical matrix-assisted laser desorption/ionization time of flight mass spectrometry (MALDI-TOF MS) spectrum of the product solution obtained by cleavage of BSA over Cu-MOF at pH 9.0 and 50°C for 50 min is illustrated in Supplementary Fig. S9. The peak of BSA disappeared in comparison with the control group (Supplementary Fig. S9a, b), and the formation of some intermediate proteins was observed (Supplementary Fig. S 9c–e). Each new MALDI-TOF MS peak represents a cleavage product obtained by proteolysis of BSA. The hydrolyzed protein fragments obtained at the peaks with m/z of 13617, 11879, 11050, 10859, 10826, 10622, 10599, 10240, 9688, 8457, 7445, 3885 and 2191. Again, MALDI-TOF MS clearly shows the cleavage of BSA by Cu-MOF.

Kinetic studies. The proteolytic activity of Cu-MOF was further examined by kinetic measurements. The rate of BSA hydrolysis was measured by SDS-PAGE in Fig. 1a and Supplementary Fig. S8. The pseudo-first-order kinetic constant (k_0) was estimated from the logarithmic plot illustrated in Fig. 2a and 2c. Within the range of the Cu-MOF concentrations considered, typical Michaelis-Menten curves were observed (50°C in Fig. 2b and 70°C in Fig. 2d) and the data were analyzed by a nonlinear regression program from which important kinetic parameters can be extracted (Table 1). The Michaelis constant, K_m is a characteristic value irrelevant to the concentrations of substrate and enzyme, and is often associated with the affinity of the catalyst molecules for the substrate[27]. The greater the K_m value is, the weaker the binding between the enzyme and substrate. The K_m value of Cu-MOF with BSA as the substrate under the optimum conditions was about 26,000-fold lower than free trypsin ($0.99 \times 10^4\ M^{-1}$)[49], suggesting that Cu-MOF has a higher affinity for BSA than trypsin. It is also significantly lower than most of the artificial metalloprotease Cu(II) complexes in Table 1.

The k_{cat} value represents the maximum number of substrate molecules turned over per catalyst molecule per unit time. It gives a direct

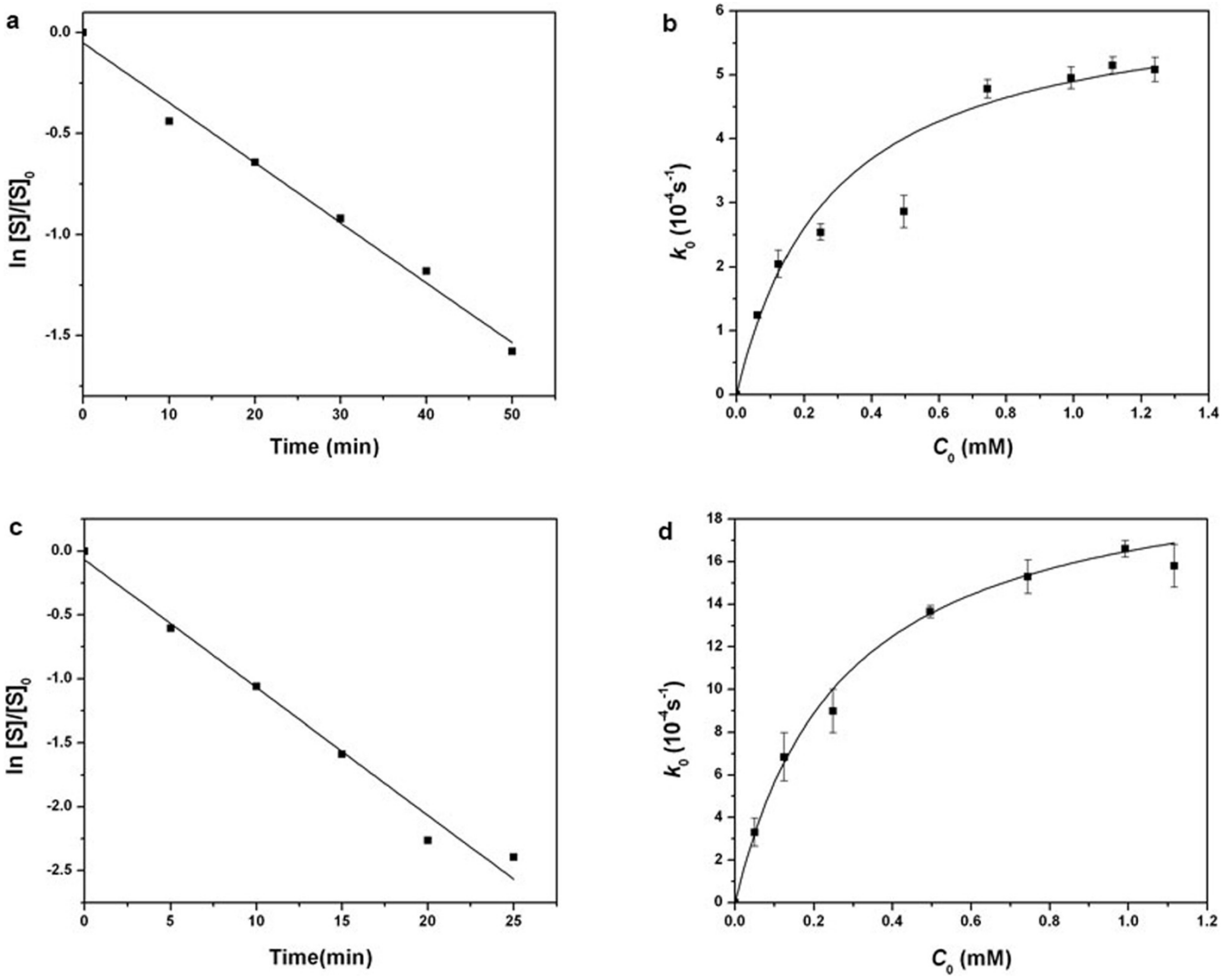

Figure 2 | **Kinetic data.** (a, c) Plot of $\ln[S]/[S]_0$ against time for the electrophoretic bands. BSA (15 μM) incubated with Cu-MOF (0.99 mM) at 50°C and 70°C respectively. The relative concentration of substrate was measured by analyzing the density of the electrophoretic bands. The straight line corresponds to k_0 of 4.95×10^{-4} s^{-1} at 50°C and 16.63×10^{-4} s^{-1} at 70°C. (b, d) Dependence of k_0 on C_0 for the cleavage of BSA at 50°C and 70°C. Data are expressed as mean ± SD of three independent experiments and analyzed by a nonlinear regression program.

measure of the catalytic activity. It can also be viewed as the optimum turnover rate[34]. The derived k_{cat} of Cu-MOF shows a value of 20.98×10^4 s^{-1} at 70°C, which is approximately four times higher than at 50°C and significantly higher than artificial metalloprotease Cu(II) complexes in Table 1. In particular, k_{cat} is 110 times higher than that of soluble Cu(II)oxacyclen catalysts[50].

Table 1 | Values of kinetic parameters for the cleavage of protein substrates by different catalysts

Catalyst	Protein	pH	Temperature (°C)	k_{cat}(10^{-4} s^{-1})	K_m(10^{-3} M^{-1})	k_{cat}/K_m($s^{-1}M^{-1}$)
Cu-MOF	BSA	9.0	50	6.28 ± 0.39	0.28 ± 0.04	2.23 ± 0.35
Cu-MOF	BSA	9.0	70	20.98 ± 0.65	0.27 ± 0.02	7.73 ± 0.68
Cu-MOF	casein	9.0	50	5.17 ± 0.56	1.16 ± 0.24	0.44 ± 0.09
Cu-MOF	casein	9.0	70	9.76 ± 0.17	0.42 ± 0.02	2.32 ± 0.12
Cu(II)A-PS[a]	BSA	9.5	50	8.0	0.92	0.87
Cu(II)B-PS[a]	BSA	9.5	50	8.7	1.2	0.73
Cu(II)oxacyclen[b]	BSA	9.5	50	0.19 ± 0.003	0.51 ± 0.03	0.036 ± 0.003
Cu(II)cyclen[b]	BSA	9.5	50	N/A	N/A	0.0005
Cu(II)C[c]	BSA	9.5	50	3.89 ± 0.56	0.11 ± 0.03	3.61 ± 0.83
Cu(II)D[c]	BSA	9.5	50	2.77 ± 0.277	0.52 ± 0.1	0.56 ± 0.11
Cu(II)E[c]	BSA	9.5	50	1.89 ± 0.17	0.17 ± 0.03	1.14 ± 0.19
Cu(II)H[c]	BSA	9.5	50	0.42 ± 0.06	0.14 ± 0.04	0.31 ± 0.083
Cu(II)I[c]	BSA	9.5	50	0.47 ± 0.06	0.53 ± 0.16	0.09 ± 0.024

N/A = data not available. a, b and c taken from ref. 18, 50, and 17, respectively. All the Cu(II) complexes except Cu(II)A- and B-PS are soluble.

The proteolytic activities of Cu-MOF and Cu(II) complexes reported in the literature were further compared in terms of k_{cat}/K_m. Interestingly, the value of k_{cat}/K_m is 2.23 s^{-1} M^{-1} at 50°C and pH 9.0 for Cu-MOF. This is much higher than that for Cu(II) complexes obtained at 50°C and pH 9.5, except for a homogeneous artificial metalloprotease Cu(II)C[17]. Particularly, the value of k_{cat}/K_m (7.73 s^{-1} M^{-1}) obtained under the optimum condition for Cu-MOF is the highest value of k_{cat}/K_m reported so far to the best of our knowledge. This value is 2 times greater than the value obtained for homogeneous artificial metalloprotease Cu(II)C and 200 times greater than that for soluble Cu(II)oxacyclen.

Reusability. As a new type of mimic enzyme, Cu-MOF could also be taken as an effective heterogeneous proteolytic reagent. Cu-MOF can be separated from the hydrolysate and used repeatedly. This gives rise to its most prominent advantages over natural enzyme. Figure 3 shows that Cu-MOF exhibited excellent reusability since it can be recycled ten times without losing a significant amount of its activity. The XRD pattern of the used Cu-MOF was almost the same as the fresh one, indicating that Cu-MOF was stable during the hydrolytic reaction (Supplementary Fig. S1). Moreover, the surface area and the pore volume of Cu-MOF only slightly decreased after reaction (Supplementary Table S1). The results confirmed that the frameworks of the Cu-MOF maintained during the proteolysis reaction.

Mechanism. The roles of Cu^{2+}, organic ligand (H_3BTC) and the Cu-MOF in the proteolytic reaction were tested and the results are shown in Fig. 4. BSA cannot be hydrolyzed in the present of only organic ligand (lane 4). The Cu^{2+} with the same concentration as containing in 0.5 mg of Cu-MOF made the BSA denaturation (lane 3 and 5). According to the results of ICP (Supplementary Table S2), the contents of Cu^{2+} released from 0.5 mg Cu-MOF in boric acid buffer (containing BSA) is about 3 $\mu g \cdot mL^{-1}$. But Cu^{2+} with this concentration had no obvious effect on BSA (lane 7). Therefore, it can be confirmed that only the coupled metal center and organic ligand, as the form of metal-organic frameworks, could catalyzed the proteolytic reaction (lane 6).

In order to ensure the protease-like activity is due to the Cu-MOF but not any component that leaches out from Cu-MOF to the reaction solution, the Cu-MOF was centrifuged out at the end of the reaction and the reaction mixture was analyze by ICP. The results are shown in Supplementary Table S2. It is found that when BSA was added, some of Cu^{2+} leached out into the solution in the first round of reaction. The amount of released Cu^{2+} decreased sharply since the second run. However, the protease activity of Cu-MOF was not depressed and it could be reused for ten times without losing a significant amount of its activity (Fig. 3). Therefore, it could be concluded that Cu-MOF plays the role of catalyst in the proteolytic reaction. Meanwhile, the FT-IR spectra of fresh and used Cu-MOF, as well as BSA are shown in Supplementary Fig. S4. Two new peaks at 620, 2950 cm^{-1} generated and the intensities of one peak at 1552 cm^{-1} enhanced after reaction. The peak at 2950 cm^{-1} and correspond to –CH stretching, which is associated with pure BSA. The stretching band at 1552 cm^{-1} shows C=O bending vibration of N–H of amide–II, respectively[51]. The peak at 620 cm^{-1} can be assigned to the wagging of NH_2 of acid amides, probably indicating the structure of protein[52]. The result mentioned above implies some interaction between Cu-MOF and BSA.

For the above reasons, a probable mechanism for catalytic hydrolysis of BSA over Cu-MOF has been proposed as following:

$$\mathrm{Cu-MOF} \xrightarrow{\mathrm{BSA}} \mathrm{Cu-MOF}* \quad (1)$$

$$\mathrm{BSA} \xrightarrow{\mathrm{Cu-MOF}*} \mathrm{hydrolysates} \quad (2)$$

In step (1), Cu-MOF reacts with bits of BSA to form a complex Cu-MOF* (i.e. recycle Cu-MOF). It is proposed that some of the framework structures on the surface of MOF crystal split and Cu^{2+} were therefore leached out, which was revealed by ICP detection. But the main structure still survived because the XRD pattern of recycle Cu-

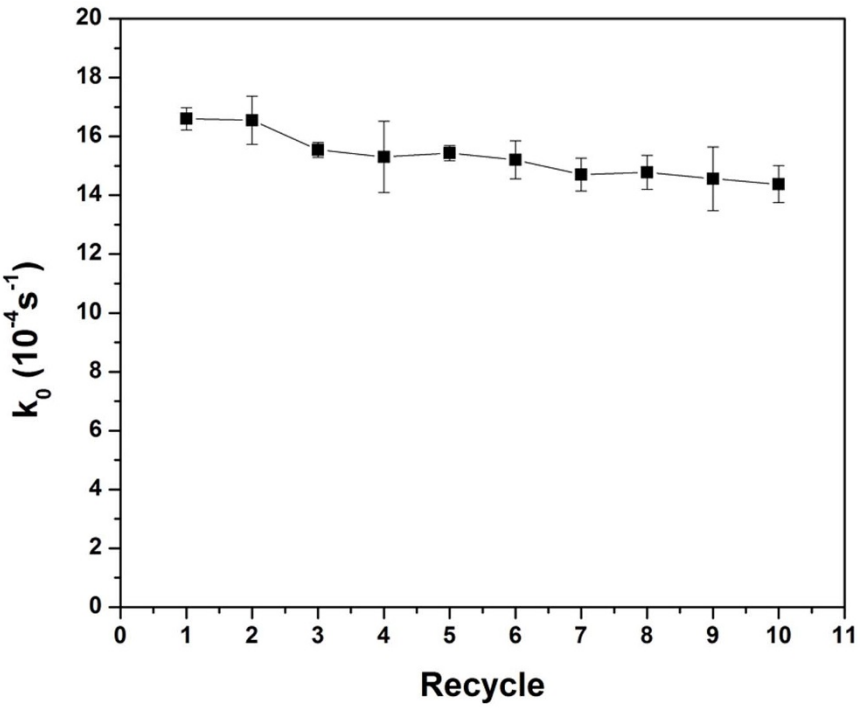

Figure 3 | Reusable experiments of Cu-MOF hydrolyzing activity. BSA (15 μM) incubated with Cu-MOF (0.99 mM) at pH 9.0 and 70°C for 25 min. Cu-MOF was recollected by centrifugation and shaken in water for 15 min. Then the catalyst was washed with ethanol three times. The solvent was removed under vacuum at 170°C for 2 h. The recycling was conducted ten times. Data are expressed as mean ± SD of three independent experiments.

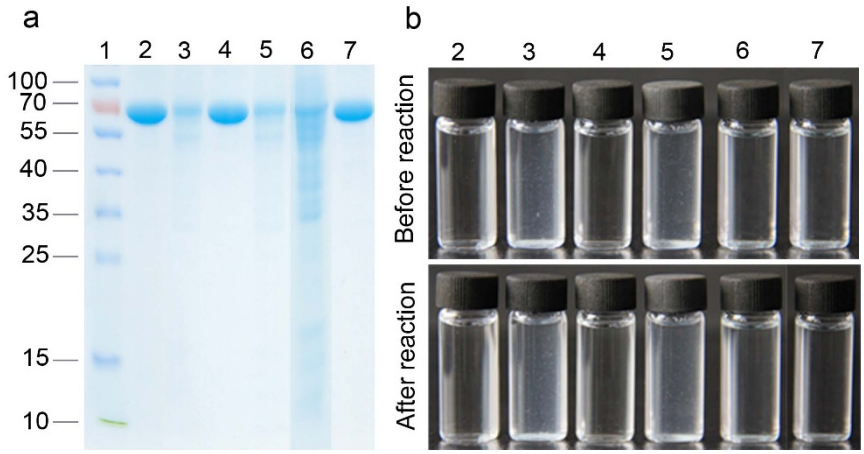

Figure 4 | (a) Results of SDS-PAGE performed on BSA (15 μM) incubated with $Cu(NO_3)_2$, Benzene-1,3,5-tricarboxylic acid (H_3BTC) and Cu-MOF (0.12 mM) for 25 min at pH 9.0 and 70°C. (b) Typical photographs of BSA solution after reaction corresponding to lanes on the SDS-PAGE left. The reaction was done in 10 mL, 50 mM boric acid buffer (pH 9.0) buffer-containing 15 μM BSA. Peptide solution was separated from the solid MOFs by centrifugation (7500 rpm, 20 min). The results were measured by sodium dodecyl sulfate polyacrylamide gel electrophoresis (SDS-PAGE). Lane 1, Marker; Lane 2, BSA; Lane 3, BSA + 0.598 mg $Cu(NO_3)_2$ (15.7 μg·mL^{-1} Cu^{2+}); Lane 4, BSA + 0.34 mg H_3BTC (34 μg·mL^{-1} H_3BTC); Lane 5, BSA + 0.598 mg $Cu(NO_3)_2$ and 0.34 mg H_3BTC; Lane 6, BSA + 0.5 mg Cu-MOF (containing 15.7 μg·mL^{-1} Cu^{2+} and 34 μg·mL^{-1} H_3BTC); Lane 7, BSA + 3 μg·mL^{-1} Cu^{2+} (according to the results of ICP, the contents of Cu^{2+} released from 0.5 mg Cu-MOF in boric acid buffer is ~3 μg·mL^{-1}).

MOF was almost the same as fresh one. Importantly, Cu-MOF* has some organic fragments from BSA on it (this could be detected by FT-IR). This make Cu-MOF* stable so Cu^{2+} no longer leached out into the solution. In step (2), Cu-MOF* could catalyze the proteolytic reaction and be reused for many times without losing in its activity. (iii) The metal center of the frameworks (Cu (II)) on the surface of the crystal should play an important role in reaction because of their strong affinity to BSA[50,53].

Cu-MOF catalyzed hydrolysis of casein. The success of using Cu-MOF to hydrolyze BSA encouraged us to extend this approach to other proteins. Since there are few reports on the synthesis of artificial proteases used for hydrolysis of casein (from bovine milk), the activity of Cu-MOF was examined further by using casein as the substrates (Supplementary Fig. S10, S11).

Casein is weakly soluble in water[54] and acidicmedia[55]. It is also very stable. For example, it can be heated to temperatures of 100°C and pressure-treated to 100 MPa without losing its essential integrity[54]. Herein, Cu-MOF can also hydrolyze casein, acting as an effective mimic enzyme with both excellent substrate binding affinity (K_m = 0.42 × 10^{-3} M^{-1}) and catalytic activity (k_{cat} = 9.76 × 10^{-4} s^{-1}) (Table 1). As expected, under the same conditions, the value of k_{cat}/K_m is 2.32 s^{-1}·M^{-1} for casein. This is about 3 times smaller than that for BSA (7.73 s^{-1} M^{-1}) (Table 1). The fact that casein is more difficult to hydrolyze than BSA suggests that it will be harder for Cu-MOF to cleave phosphoproteins than non-phosphoproteins.

Cu-MOF simulated the trypsinizationin cell culture. Trypsin is an essential reagent for routine cell culture work. And EDTA is usually required with trypsin solutions as a chelating agent with gentle dissociative properties that acts to increase trypsin efficiency by neutralizing calcium and magnesium ions because calcium and magnesium ions enhance the cell-to-cell adhesion and obscure the peptide bonds on which trypsin acts and separates the cells[56]. Interestingly, the trypsinization in Lung cancer A549 cells culture could be simulated by using Cu-MOF even without EDTA. There were barely Cu^{2+} ions (<0.0003 wt%) release from Cu-MOF in pH 7.4 buffer (Supplementary Table S2), which implies Cu-MOF is stable. Under the phase contrast microscope, A549 cells were spread well and fusiform or polygonal with clear outlines and smooth edges (Fig. 5a, d). After they were treated by using 0.1% Cu-MOF for 10 min at 37°C, the edges of A549 cells shrank and became round or even detached from the bottom (Fig. 5b), which was similar to those cells treated with trypsin-EDTA (0.25% trypsin with 0.02% EDTA) for 2 min at 37°C (Fig. 5c). When these treated A549 cells were further cultured for 24 h with fresh medium at 37°C, they spread well and the cell membranes were not affected (Fig. 5e, f). Furthermore, crystal violet staining of these Cu-MOF treated cells showed that A549 cells attached to the plates again and spread well (Fig. 5h) which was similar to those treated with trypsin (Fig. 5i) and control group (Fig. 5g), suggesting the good recovery of normal cells shape. Although the treated time by using Cu-MOF was longer than that using trypsin, the concentration of Cu-MOF was much lower and no EDTA was needed.

Discussion

The present study demonstrates that Cu-MOF has excellent hydrolysis efficiency and stability upon reuse. It can greatly increase the enzymatic activity and stability even at extreme conditions such as very high pH and temperatures. Moreover, Cu-MOF was successfully used to simulate trypsinization in cell culture since it dissociated cells in culture even without EDTA. Although these findings are not clearly understood yet, the high efficient proteolytic activity of Cu-MOF could be attributed to some synergistic effects between the following properties: a large specific surface area and stable well-defined crystalline open structure provides the unique hosting ability of MOF to BSA molecules; also, the space confinement effect of MOF mesopores to biomacromolecules mimics the cage-like nature of an enzyme's active site[37,57]. The unsaturated Cu(II) sites could also be beneficial for the preferential interactions between BSA molecules and Cu-MOF.

Moreover, during the simulation of trypsinization in cell culture, it is unclear if the growth- and metabolism-related protein expression levels and the apoptosis-related protein expression levels were affected by Cu-MOF. This is worth further investigation in the future.

These findings and previous peroxidase mimics findings[27–29] induce us to call them "MOFzymes" in analogy to the nomenclature of "nanozymes"[10,11]. In the context of their application in the field of proteomics, the availability of various building blocks consisting of metals and organic linkers makes it possible to construct a variety of custom-designed powerful MOFs of which Cu-MOF is just a prototype with intrinsic enzyme-like activities for the specific substrates.

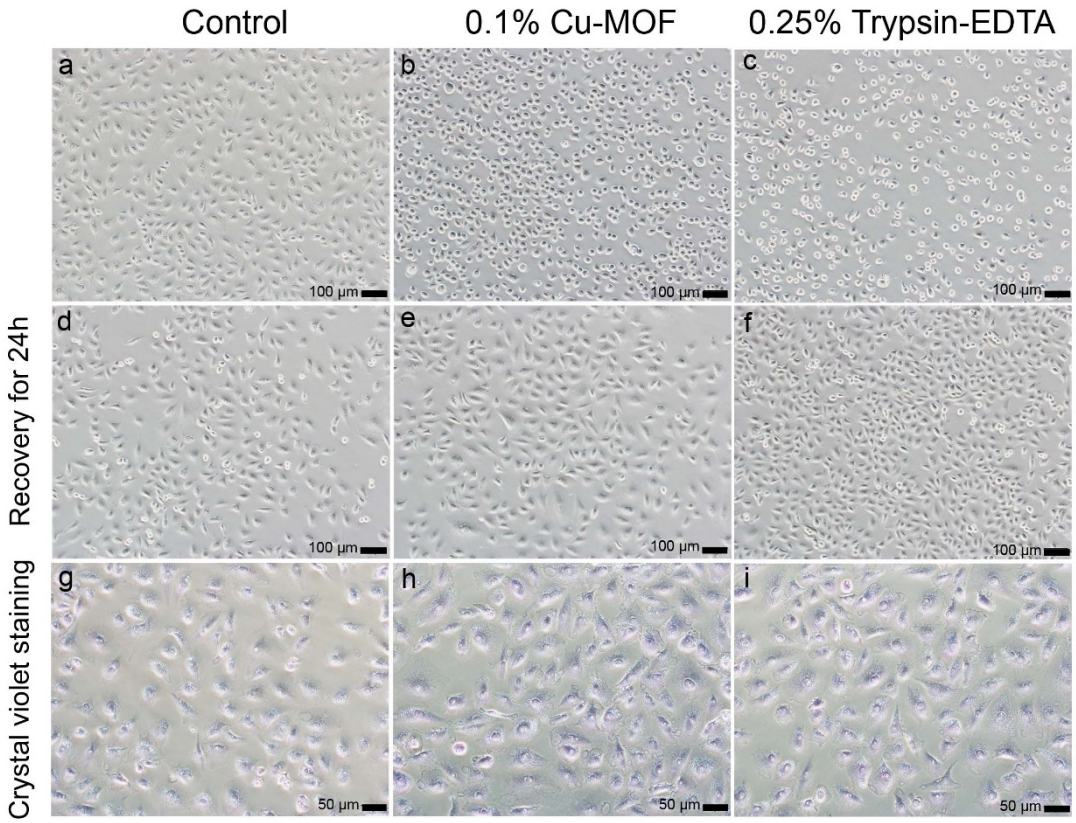

Figure 5 | Influence of Cu-MOF on A549 cells morphological changes. (a–f) Morphological changes in A549 cells treated with Cu-MOF and trypsin-EDTA followed by recovery for 24 h. (a, d) control group. (b) 0.1% Cu-MOF, 10 min. (c) 0.25% trypsin-0.02% EDTA, 2 min. (e, f) recovery 24 h. (g–i) Morphological changes in A549 cells treated with Cu-MOF in crystal violetstaining.

In conclusion, the synthesized Cu-MOF with the microporous network and typical octahedral crystals possesses highly efficient intrinsic protease-like activity, catalyzing the proteins (BSA and casein) at aqueous solution and keep great stability during the reaction. Furthermore, Cu-MOF exhibits good stability during hydrolyzing reaction and can be reused for ten times without losing a significant amount of its activity. Although detailed mechanistic information is not available, the present study demonstrates that Cu-MOF possibly could react with BSA to form a complex Cu-MOF*, which has some organic fragments from BSA on it. Interestingly, Cu-MOF is successfully used in cell dissociation without EDTA. These findings mentioned above will open an avenue for using metal-organic frameworks as an artificial protease.

Methods

Chemicals and instrumentation. Benzene-1, 3, 5-tricarboxylic acid was purchased from Aldrich. Copper(II) nitrate hemientahydrate, *N,N*-dimethylformamide, ethanol and dichloromethane were purchased from Fisher. Bovine serum albumin, casein, trypsin, penicillin, streptomycin and crystal violet were purchased from Sigma. RPMI1640 medium and fetal bovine serum was purchased from Hyclone. All commercial chemicals were used without further purification. Fourier transform infrared measurements were performed on a Nicolet 8700 Instrument. X-ray powder diffraction (XRD) experiments were conducted on a D/max-3B spectrometer with Cu Kα radiation. Scans were made in the 2θ range 3–80° with a scan rate of 10° min^{-1} (wide angle diffraction). Pore size distributions, BET surface areas and pore volumes were measured by nitrogen adsorption/desorption measurements using a Micromeritics Tristar II Surface area and porosity analyzer. Prior to the analysis, the samples were degassed at 90°C for 1 h. Scanning electron microscopy (SEM) images of the samples were taken on a FEI Quanta 200FEG microscope. Inductively coupled plasma–atomic emission spectrometry (ICP–AES) analysis was used to determine the contents of Cu^{2+} released from Cu-MOF. ICP-AES measurement was carried out with a Shimadzu ICPS-1000IV model. A549 cells visualized using an Olympus IX73 microscope.

Synthesis of Cu-MOF. In a typical synthesis, 5.0 g (24 mM) Benzene-1, 3, 5-tricarboxylic acid and 10 g (43 mM) copper (II) nitrate hemipentahydrate were dissolved in 250 mL of solvent consisting of equal parts *N, N*-dimethylformamide, ethanol and deionized water. The solution was filled in a 1 L wide mouth glass jar and heated at 90°C for 20 h. After cooling, the product in the solution was filtered off to remover excessive reactants, washed with DMF and immersed in dichloromethane for 3 d. The fresh dichloromethane was replenished three times and removed under vacuum at 170°C. The pure Cu-MOF was obtained.

Sample preparation. Distilled and de-ionized water was used for preparation of buffer solutions. Buffers (50 mM) used in this study were phosphate buffered saline (pH 7.4) and boric acid buffer (pH 8.0–9.0). All buffer solutions were filtered with 0.45 μm Millipore microfilter before use. All tests used fresh solutions. The resulting protein solution was stored at −20°C before use.

Effect of pH on catalytic hydrolysis of BSA. Experiments on the effect of pH were performed at a fixed temperature (50°C). BSA dissolved in 50 mM phosphate buffered saline (pH 7.4) and boric acid buffers (pH 8.0–9.0) were filtered with 0.45 μm Millipore microfilters. The pH measurements were carried out with a Lei ci pHS-25 pH/Ion meter. The concentration of BSA was 15 μM. Then Cu-MOF (1.24 mM) was added to 10 mL BSA solution and reacted for 50 min. After the incubation, hydrolysate was subjected to SDS-PAGE. The degree of hydrolysis on BSA was determined by the plot of $-\ln[S]/[S]_0$ against time.

Proteolysis reactions. The BSA solution (15 μM, 10 mL) was added to the Cu-MOF with gentle vortex mixing, and then the activity of Cu-MOF was measured at pH 9.0, the temperature from 37 to 70°C, and the time from 0 to 5 h. The Cu-MOF concentration was 0.99 mM. The reaction results were collected at a shaking speed of 180 rpm. The peptide solution was separated from the solid MOFs by centrifugation for 20 min. For the enzyme control, digestion was performed by adding trypsin to the pretreated protein sample with a substrate-to-enzyme ratio of 40 : 1 (w/w). After different reaction times, 0.5 mL hydrolysate was drawn from the reactor system and centrifuged at 7500 rpm for 20 min. The products were separated by denaturing polyacrylamide gel electrophoresis (SDS-PAGE) with a Cleaver SD10 model. The rate of protein cleavage was measured by monitoring the decrease in the intensity of the electrophoretic bands and MALDI-TOF MS. The densities of the electrophoretic bands were analyzed with an Alpha View SA model. MALDI-TOF MS analysis was carried out with an autoflex speed reflection model and a linear model. The kinetic data were measured at various C_0 (0 ~ 1.24 mM) at the optimum pH 9.0 and temperatures of 50 and 70°C. The degree of cleavage of proteins was measured by SDS-PAGE.

Hydrolysis of casein. The proteolytic reaction with 1 $mg \cdot mL^{-1}$ casein substrate was performed at 50°C and 70°C, with a pH 9.0. Rate data were collected by varying the amount of Cu-MOF (0 ~ 1.74 mM). After different reaction times, 0.5 mL hydrolysate was drawn from the reactor system and centrifuged at 7500 rpm for 20 min. The protein in clear liquid was examined by SDS-PAGE. The rate of protein cleavage was measured by monitoring the decrease in the intensity of the electrophoretic bands corresponding to casein.

Reuse of Cu-MOF. The proteolytic reaction was performed at 70°C and pH 9.0. Cu-MOF (0.99 mM) was added to BSA solution (15 μM). Every 5 min, 0.5 mL hydrolysate was withdrawn from the reaction system and centrifuged at a speed of 7500 rpm for 20 min. Then the protein in clear liquid was examined by SDS-PAGE. To evaluate the reusability of Cu-MOF, the insoluble catalyst was recycled after the catalytic reaction. Cu-MOF was recollected by centrifugation and shaken in water for 15 min. Then the catalyst was washed with ethanol three times. The solvent was removed under vacuum at 170°C for 2 h. The recycling was conducted ten times.

Cancer cell line and culture. The human non-small cell lung carcinoma (A549) cell line was purchased from the American Type Culture Collection (ATCC). The cells were grown in RPMI1640 medium supplemented with 10% fetal bovine serum, 100 Units mL^{-1} penicillin and 10 $mg \cdot mL^{-1}$ streptomycin at 37°C in a humidified incubator with 5% CO_2.

Cu-MOF simulated the trypsinization and cell recovery. A549 cells (1×10^4/well) were seeded on 35 mm dish. Once 80% of confluence is reached, A549 cells were washed with PBS. 0.1% Cu-MOF and 0.25% trypsin-0.02% EDTA were added to the culture medium and cells were incubated for 10 min and 2 min, respectively. Afterwards cells were washed with PBS buffer and then visualized using an Olympus IX73 microscope. Then cells added fresh medium and incubated 24 h.

Cell staining. After treated with 0.1% Cu-MOF, cells were washed with PBS buffer and fixed with 4% ice-cold paraformaldehyde for 10 min, washed in de-ionized water once and stained with 0.25% crystal violet at room temperature for 15 min. Afterwards cells were carefully washed with de-ionized water three times and then visualized using Olympus IX73 microscope.

1. Mina, K., Kim, J., Park, K. & Yoo, Y. J. Enzyme immobilization on carbon nanomaterials: Loading density investigation and zeta potential analysis. *J. Mol. Catal. B-Enzym.* **83**, 87–93 (2012).
2. Krajewska, B. Application of chitin- and chitosan-based materials for enzyme immobilizations: a review. *ZnzymeMicrob. Tech.* **35**, 126–139 (2004).
3. Ali, S. S. *et al.* A biologically effective fullerene (C_{60}) derivative with superoxide dismutase mimetic properties. *Free Radical Biol. Med.* **37**, 1191–1202 (2004).
4. Pasquato, L., Rancan, F., Scrimin, P., Mancin, F. & Frigeri, C. N-methylimidazole-functionalized gold nanoparticles as catalysts for cleavage of a carboxylic acid ester. *Chem. Commun.* **17**, 2253–2254 (2000).
5. Comotti, M., Pina, C. D., Matarrese, R. & Rossi, M. The catalytic activity of "naked" gold particles. *Angew. Chem. Int. Ed.* **43**, 5812–5815 (2004).
6. Chen, J., Patil, S., Seal, S. & McGinnis, J. F. Rare earth nanoparticles prevent retinal degeneration induced by intracellular peroxides. *Nat. Nanotechnol.* **1**, 142–150 (2006).
7. Gao, L. *et al.* Intrinsic peroxidase-like activity of ferromagnetic nanoparticles. *Nat. Nanotechnol.* **2**, 577–583 (2007).
8. Wei, H. & Wang, E. Fe_3O_4 magnetic nanoparticles as peroxidase mimetics and their applications in H_2O_2 and glucose detection. *Anal. Chem.* **80**, 2250–2254 (2008).
9. Fan, K. *et al.* Magnetoferritin nanoparticles for targeting and visualizing tumour tissues. *Nat. Nanotechnol.* **7**, 459–464 (2012).
10. Manea, F., Houillon, F. B., Pasquato, L. & Scrimin, P. *Nanozymes: Gold-nanoparticle-based transphosphorylation catalysts. Angew. Chem. Int. Ed.* **43**, 6165–6169 (2004).
11. Pasquato, L., Pengo, P. & Scrimin, P. Nanozymes: Functional nanoparticle-based catalysts. *Supramol. Chem.* **17**, 163–171 (2005).
12. Hegg, E. L. & Burstyn, J. N. Hydrolysis of unactivated peptide bonds by a macrocyclic copper(II)complex: Cu([9]aneN_3)Cl_2 hydrolyzes both dipeptides and proteins. *J. Am. Chem. Soc.* **117**, 7015–7016 (1995).
13. Kim, H. M., Jang, B., Cheon, Y. E., Suh, M. P. & Suh, J. Proteolytic activity of Co(III) complex of 1-oxa-4,7, 10-triazacyclododecane: a new catalytic center for peptide-cleavage agents. *J. Biol. Inorg. Chem.* **14**, 151–157 (2009).
14. Wang, X., Wang, D., Liang, P. & Liang, X. Synthesis and properties of an insoluble chitosan resin modified by azamacrocycle copper(II) complex for protein hydrolysis. *J. Appl. Polym. Sci.* **128**, 3280–3288 (2013).
15. Kassai, M., Ravi, R. G., Sarah, S. J. & Grant, K. B. Unprecedented acceleration of zirconium(IV)-assisted peptide hydrolysis at neutral pH. *Inorg. Chem.* **43**, 6130–6132 (2004).
16. Yashiro, M., Kawakami, Y., Taya, J., Arai, S. & Fujii, Y. Zn(II) complex for selective and rapid scission of protein backbone. *Chem. Commun.* **12**, 1544–1546 (2009).
17. Kim, M. G. *et al.* Soluble artificial metalloproteases with broad substrate selectivity, high reactivity, and high thermal and chemical stabilities. *J. Biol. Inorg. Chem.* **15**, 1023–1031 (2010).
18. Yoo, S. H., Lee, B. J., Kim, H. & Suh, J. Artificial metalloprotease with active site comprising aldehyde group and Cu(II)Cyclen complex. *J. Am. Chem. Soc.* **127**, 9593–9602 (2005).
19. Ma, S. Gas adsorption applications of porous metal–organic frameworks. *Pure Appl. Chem.* **81**, 2235–2251 (2009).
20. Lee, J. *et al.* Metal–organic framework materials as catalysts. *Chem. Soc. Rev.* **38**, 1450–1459 (2009).
21. Rowsell, J. L. C. & Yaghi, O. M. Effects of functionalization, catenation, and variation of the metal oxide and organic linking units on the low-pressure hydrogen adsorption properties of metal-organic frameworks. *J. Am. Chem. Soc.* **128**, 1304–1315 (2006).
22. Gu, Z.-Y., Park, J., Raiff, A., Wei, Z. & Zhou, H.-C. Metal–Organic Frameworks as Biomimetic Catalysts. *ChemCatChem* **6**, 67–75 (2014).
23. Falcaro, P. *et al.* A new method to position and functionalize metal-organic framework crystals. *Nat. Commun.* **2**, 237 (2011).
24. Sun, C.-Y. *et al.* Efficient and tunable white-light emission of metal–organic frameworks by iridium-complex encapsulation. *Nat. Commun.* **4**, 2717 (2013).
25. Yu, J. *et al.* Confinement of pyridiniumhemicyanine dye within an anionic metal-organic framework for two-photon-pumped lasing. *Nat. Commun.* **4**, 2719 (2013).
26. Mammen, M., Choi, S.-K. & Whitesides, G. M. Polyvalent interactions in biological systems: implications for design and use of multivalent ligands and inhibitors. *Angew. Chem. Int. Ed.* **37**, 2754–2794 (1998).
27. Feng, D. *et al.* Zirconium-metalloporphyrin PCN-222: mesoporous metal–organic frameworks with ultrahigh stability as biomimetic catalysts. *Angew. Chem. Int. Ed.* **51**, 10307–10310 (2012).
28. Ai, L., Li, L., Zhang, C., Fu, J. & Jiang, J. MIL-53(Fe): a metal-organic framework with Intrinsic peroxidase-like catalytic activity for colorimetric biosensing. *Chem. Eur. J.* **19**, 15105–15108 (2013).
29. Zhang, J. W. *et al.* Water-stable metal–organic frameworks with intrinsic peroxidase-like catalytic activity as a colorimetric biosensing platform. *Chem. Commun.* **50**, 1092–1094 (2014).
30. Gu, Z.-Y., Chen, Y.-J., Jiang, J.-Q. & Yan, X.-P. Metal–organic frameworks for efficient enrichment of peptides with simultaneous exclusion of proteins from complex biological samples. *Chem. Commun.* **47**, 4787–4789 (2011).
31. Jung, S. *et al.* Bio-functionalization of metal-organic frameworks by covalent protein conjugation. *Chem. Commun.* **47**, 2904–2906 (2011).
32. Lykourinou, V. *et al.* Immobilization of MP-11 into a mesoporous metal-organic framework, MP-11@mesoMOF: a new platform for enzymatic catalysis. *J. Am. Chem. Soc.* **133**, 10382–10385 (2011).
33. Chen, Y., Lykourinou, V., Hoang, T., Ming, L.-J. & Ma, S. Size-selective biocatalysis of myoglobin immobilized into a mesoporous metal−organic framework with hierarchical pore sizes. *Inorg. Chem.* **51**, 9156–9158 (2012).
34. Larsen, R. W. *et al.* Mimicking heme enzymes in the solid state: metal-organic materials with selectively encapsulated heme. *J. Am. Chem. Soc.* **133**, 10356–10359 (2011).
35. Qin, F.-X. *et al.* Hemin@metal-organic framework with peroxidaselike activity and its application to glucose detection. *Catal. Sci. Technol.* **3**, 2761–2768 (2013).
36. Shih, Y.-H. *et al.* Novel trypsin-FITC@MOF bioreactor efficiently catalyzes protein digestion. *ChemPlusChem.* **77**, 982–986 (2012)
37. Liu, W.-L. *et al.* Trypsin-immobilized metal–organic framework as a biocatalyst in proteomics analysis. *J. Mater. Chem. B* **1**, 928–932 (2013).
38. Jang, B.-B., Lee, K.-P., Min, D.-H. & Suh, J. Immobile artificial metalloproteinase containing both catalytic and binding groups. *J. Am. Chem. Soc.* **120**, 12008–12016 (1998).
39. Majano, G. & Pérez-Ramírez, J. Scalable room-temperature conversion of copper(II) hydroxide into HKUST-1 ($Cu_3(btc)_2$). *Adv. Mater.* **25**, 1052–1057 (2013).
40. Peterson, G. W., DeCoste, J. B., Grant Glover, T., Huang, Y., Jasuja, H. & Walton, K. S. Effects of pelletization pressure on the physical and chemical properties of the metal–organic frameworks $Cu_3(BTC)_2$ and UiO-66. *Micropor. Mesopor. Mat.* **179**, 48–53 (2013).
41. Kim, J., Cho, H.-Y. & Ahn, W.-S. Synthesis and adsorption/catalytic properties of the metalorganic framework CuBTC. *Catal. Surv. Asia* **16**, 106–119 (2012).
42. Chui, S. S. Y., Lo, S. M. F., Charmant, J. P. H., Orpen, A. G. & Williams, I. D. A chemically functionalizable nanoporousmaterial $[Cu_3(TMA)_2(H_2O)]_3$n. *Science* **283**, 1148–1150 (1998).
43. Schlichte, K., Kratzke, T. & Kaskel, S. Improved synthesis, thermal stability and catalytic properties of the metal-organic framework compound $Cu_3(BTC)_2$. *Micropor. Mesocpor. Mat.* **73**, 81–88 (2004).
44. Petit, C., Burress, J. & Bandosz, T. J. The synthesis and characterization of copper-based metal–organic framework/graphite oxide composites. *Carbon* **49**, 563–572 (2011).
45. Vairam, S. & Govindarajan, S. New hydrazinium salts of benzene tricarboxylic and tetracarboxylicacid–spreparation and their thermal studies. *Thermochimica Acta* **414**, 263–270 (2004).
46. Kim, H. *et al.* Effective artificial proteases synthesized by covering silica gel with aldehyde and various other organic groups. *Bioorg. Med. Chem. Lett.* **12**, 3247–3250 (2002).
47. Yoo, C. E., Chae, P. S., Kim, J. E., Jeong, E. J. & Suh, J. Degradation of myoglobin by polymeric artificial metalloproteases containing catalytic modules with various

catalytic group densities: site selectivity in peptide bond cleavage. *J. Am. Chem. Soc.* **125**, 14580–14589 (2003).
48. Suh, J. & Oh, S. Remarkable proteolytic activity of imidazoles attached to cross-linked polystyrene. *J. Org. Chem.* **65**, 7534–7540 (2000).
49. Ram, J. S. & Maurer, P. H. Modified bovine serum albumin. III. hydrolysis studies with trypsin, chymotrypsin and pepsin. *Arch. Biochem. Biophys.* **70**, 185–204 (1957).
50. Jang, S. W. & Suh, J. Proteolytic activity of Cu(II) complex of 1-Oxa-4,7,10-triazacyclododecane. *Org. Lett.* **10**, 481–484 (2008).
51. Swain, S. K. & Sarkar, D. Study of BSA protein adsorption/release on hydroxyapatite nanoparticles. *Appl. Surf. Sci.* **286**, 99–103 (2013).
52. Zeng, G. *et al.* Effect of monorhamnolipid on the degradation of n-hexadecane by Candida tropicalis and the association with cell surface properties. *Appl. Microbiol. Biotechnol.* **90**, 1155–1161 (2011).
53. Patra, A. *et al.* Synthesis, structure, spectroscopic characterization, and protein binding affinity of new water-soluble hetero- and homometallic tetranuclear $[Cu_2Zn^{II}_2]$ and $[Cu^{II}_4]$ Clusters. *Inorg. Chem.* **52**, 2880–2890 (2013).
54. Dalgleish, D. G. On the structural models of bovine casein micelles-review and possible improvements. *Soft Matter* **7**, 2265–2272 (2011).
55. Jollès, P. Progress in the chemistry of casein. *Angew. Chem. Int. Edit.* **6**, 558–566 (1966).
56. Olsen, J. V., Ong, S. E. & Mann, M. Trypsin cleaves exclusively C-terminal to arginine and lysine residues. *Mol. Cell Proteomics* **3**, 608–614 (2004).
57. Wiester, M. J., Ulmann, P. A. & Mirkin, C. A. Enzyme mimics based upon supramolecular coordination chemistry. *Angew. Chem. Int. Ed.* **50**, 114–137 (2011).

Acknowledgments

The authors thank National Natural Science Foundation of China (Project 21367024, 21464016, 21403190, 21263027, NSFC-YN U1033603) and the Program for Innovative Research Teams (in Science and Technology) in the University of Yunnan Province and Key project from Yunnan Educational Committee for financial support.

Author contributions

B.L. and J.W. conceived the idea, supervised all aspects of this project and contributed to the paper. D.C. carried out the major part of biochemical experiments, analyzed the data and contributed to the paper. Z.Y. and L.J. carried out part of the biochemical experiments together with D.D. They and J.H. analyzed the data, was involved in discussions, critical assessment, and manuscript improvements. Z.L., F.Y. and J.Z. synthesized and characterized the MOF samples.

Additional information

Supplementary information accompanies this paper at http://www.nature.com/scientificreports

Competing financial interests: The authors declare no competing financial interests.

How to cite this article: Li, B. *et al.* MOFzyme: Intrinsic protease-like activity of Cu-MOF. *Sci. Rep.* **4**, 6759; DOI:10.1038/srep06759 (2014).